

Haverford College

Haverford Scholarship

Faculty Publications

Physics

1997

Cluster formation due to collisions in granular material

A. Kudrolli

M. Wolpert

Jerry P. Gollub
Haverford College

Follow this and additional works at: https://scholarship.haverford.edu/physics_facpubs

Repository Citation

"Cluster Formation due to Collisions in Granular Material", A. Kudrolli, M. Wolpert, and J.P. Gollub, Phys. Rev. Lett. 78, 1383 (1997).

This Journal Article is brought to you for free and open access by the Physics at Haverford Scholarship. It has been accepted for inclusion in Faculty Publications by an authorized administrator of Haverford Scholarship. For more information, please contact nmedeiro@haverford.edu.

Cluster Formation due to Collisions in Granular Material

A. Kudrolli, M. Wolpert, and J. P. Gollub

*Physics Department, Haverford College, Haverford, Pennsylvania 19041
and Department of Physics, University of Pennsylvania, Philadelphia, Pennsylvania 19104*

(Received 9 September 1996)

The role of inelastic collisions in granular hydrodynamics is studied experimentally in a two dimensional system of spherical particles rolling on a smooth surface and driven by a moving wall. Clusters form at high particle densities; the velocity distribution is narrowed, and the collision rate is enhanced within the clusters. The clusters migrate downward in the presence of a very slight tilt, but are not dispersed. A one dimensional model captures the effect of gravitation on the observed statistical distributions. [S0031-9007(97)02416-2]

PACS numbers: 83.70.Fn, 05.20.Dd, 46.10.+z, 83.10.Pp

Granular flows give rise to a variety of phenomena that have both fluid and solid aspects [1,2]. Recently, considerable attention has been devoted to the role of inelastic collisions in granular flow. Numerical and theoretical work on particles that are allowed to “cool” due to inelastic collisions reveals “inelastic collapse” (an infinite number of collisions in a finite time) [3,4]. In two dimensions, string-like structures are produced [5]. The role of inelasticity has also been studied in a steady state situation where the particles are in contact with an energy reservoir [6]. Most of the particles are observed to form slowly moving clusters, while a few have high velocities, thus violating equipartition of energy. Recently, “temperature” and density profiles (as a function of distance from the energy source) and velocity distributions have been considered theoretically in two dimensions, in the nearly elastic limit [7]. Understanding the role of inelastic collisions may eventually be useful in elucidating the fascinating macroscopic properties displayed by granular flows, such as convection, parametric wave propagation, and size segregation [8–10].

In this Letter we present an experiment that addresses the role of inelastic collisions. The system consists of 100–2000 steel spheres rolling on a smooth bounded rectangular surface; one of the side walls is displaced periodically to supply energy. This system has several additional effects such as rolling and sliding friction that have not yet been studied theoretically. The surface can also be tilted slightly (upward from the driving wall) so that gravitation can be made either important or insignificant.

We observe strong aggregation or clustering of particles as their number is increased. We study this phenomenon statistically by measuring probability distributions for particle density and particle velocity as a function of particle number N , rate of energy input, distance from the energy source, and angle of inclination θ . The clustering occurs far from the moving wall for $\theta = 0$, and near it for small positive angles. These phenomena are also observed numerically by extending the one-dimensional model of Ref. [6] to include gravity. The presence of clusters leads to a reduction in the mean velocity and a strong narrowing of the velocity distribution. Within the clusters, the colli-

sion rate is enhanced. When clusters are produced near the periodically moving wall, parametric hydrodynamic instabilities and other collective effects appear.

The experiment consists of 3.2 mm diameter stainless steel particles rolling on a Delrin surface that was machined and polished to a uniformity of 0.001 cm. Delrin was chosen because of its low coefficient of rolling friction with steel ($\mu_r \approx 2.0 \times 10^{-3}$). The coefficient of restitution r for the steel particles is 0.93 ± 0.02 ; this value was obtained by bouncing particles on a stainless steel block and is similar to values reported elsewhere [11]. The fixed sidewalls of the apparatus are made of stainless steel, and the driving wall is made of Garolite [12]. The length L of the system perpendicular to the moving wall can be adjusted. In the data presented here, a 30 cm \times 30 cm area is used, but similar results are obtained when the area is reduced. The positions of the particles are obtained using a Dalsa CCD variable scan camera that captures 512×512 pixel images with an adjustable exposure time.

The driving wall is moved through a fixed distance of 1 cm using two computer controlled solenoids that push the sidewall and one that returns it. (An impulsive force allows larger particle velocities than does sinusoidal forcing.) The velocity v_w of the wall increases monotonically during its displacement: $v_w \approx (ad^2 + bd)^{1/2}$, where a and b are constants. The velocity that a particle acquires during its collision with the wall depends both on its initial velocity and on the instant of the collision within the driving cycle. As a result, the distribution of particle velocities generated by the external source is broad, and its mean value can be selected.

Sample images are shown in Fig. 1 of the particle distribution for $N = 100$ and 1860; the driving wall is located at the lower edge of the figure. Because of residual friction, it is necessary to tilt the surface very slightly (0.05°) in order to obtain sustained motion; this ensures that some of the particles are struck by the driving wall during each cycle. The particles appear bright against a dark background. In the case $N = 100$, the particles appear to be distributed randomly in space, and few are at rest. On the other hand, for $N = 1860$ the particles

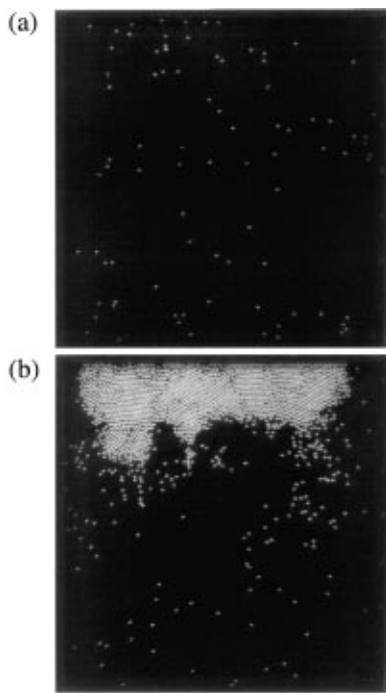


FIG. 1. Sample images showing a random distribution of particles at low total particle number N , and clustering at higher N . The driving wall is at the bottom. (a) $N = 100$; (b) $N = 1860$.

cluster near the side opposite the driving wall as can be seen from Fig. 1(b). The particles in the highly clustered region have very small velocities, but those between the clustered particles at the top and the driving walls move rapidly. Some particles that strike the driving wall emerge with very high velocities (up to 200 cm/s in some cases) and scatter many times from the other particles, rapidly transferring energy to them. The incident particle may become part of the cluster while others are released from it. The cluster contains both regular crystals and disordered regions. It is possible that interparticle friction enhances the stability of the cluster. Finally, if the driving is suddenly switched off, particles collide a few times and then come to rest, but clustered domains persist.

To extract the positions of the particles automatically, we use first a threshold intensity to locate the spots associated with the particles and to discriminate against noise. We then locate pixels within the spots that are intensity maxima in both x and y directions. Occasionally, multiple maxima within a single spot occurs; these duplicates are detected and their positions averaged. This scheme correctly detects about 97% of the particles. By analyzing a large number of images, a statistical ensemble is produced. The probability distribution function $P(n)$ of the local particle number n [and also the spatial concentration variation $n(y)$ as a function of position y from the energy source] can be extracted. To obtain both of these quantities, we divide the image of the enclosure into small boxes (typically $L/16$ or $L/32$ on a side) and determine

the occupation probability for different numbers n of particles in a box.

The density distributions $P(n)$ are plotted in Fig. 2(a) for three different total numbers N of particles. For low N (e.g., $N = 100$), the distribution is not far from a Poisson distribution, as would be expected if there are no correlations. As N is increased, the distribution shifts to larger number density n . For $N = 500$ or more, a clear peak is visible in $P(n)$; this is the hallmark of the clustering seen in Fig. 1. The cutoff of the distribution is approximately equal to the value of n for close packing. Approximately 400–500 particles are required to produce strong clustering. This estimate is not changed significantly by a factor of 2 reduction in L , but the transition is fairly broad.

The spatial density variation $n(y)$ as a function of distance from the driving wall is plotted in Fig. 2(b). One clearly sees that the particles are more or less uniformly distributed for low N , and that a peak develops progressively near the far wall as N is increased. (The apparent reduction in the peak size for large N is a consequence of the normalization factor.)

Next we discuss a case where the table is tilted slightly further to 0.22° , a value sufficient to counteract rolling friction so that all the particles move to the driving wall when the forcing is switched off. For $N = 100$, forcing causes the particles again to be randomly distributed as in the previous case shown in Fig. 1. However, as N is increased to about 500, clustering again occurs, but in this case *near* the energy source. An example for $N = 1000$ is shown in Fig. 3. For a constant driving force, the location of the clusters varies strongly (but smoothly) from the far wall to the driving wall as the angle of inclination is increased from 0.05° to 0.2° . In addition, the particles display

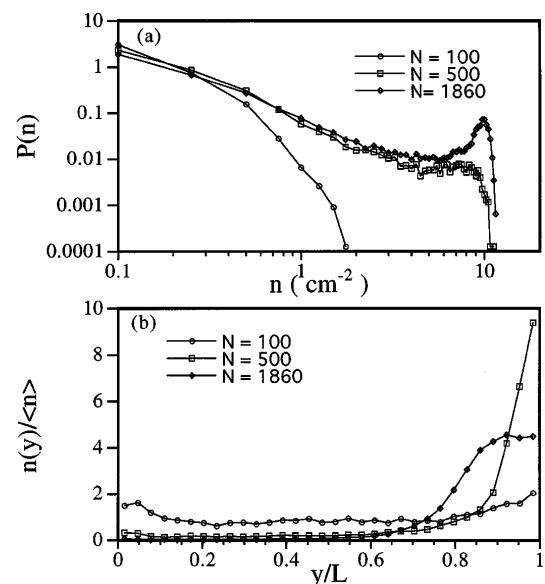


FIG. 2. (a) Probability distributions of the local number density, $P(n)$, for three different values of N . (b) Spatial density variation $n(y)$, normalized by the global density $\langle n \rangle$, as a function of distance y from the driving wall. Lines join the data points.



FIG. 3. Sample image for $N = 1000$ particles, showing strong clustering near the driving wall. When the surface is tilted by $\theta = 0.22^\circ$ upwards from the cluster.

archlike structures that oscillate subharmonically. A similar effect has been seen in vertically vibrated granular material [13,14]. In Fig. 3, the driving is sufficient to produce peak velocities of 50 cm/s. The clusters are seen even at much higher forcing amplitudes, for which the typical kinetic energy acquired at the system boundary is an order of magnitude greater than the gravitational potential energy. The density distributions $P(n)$ and spatial density variation $n(y)$ are shown for this slightly inclined case in Fig. 4. The density distributions are quite similar to those of Fig. 2, but of course $n(y)$ peaks for small y instead of for large y . The upward shift in the peak in $n(y)$ at the highest value of N is a result of the finite particle size.

A full picture of these phenomena requires speed distributions $P(v)$. These can be accurately measured using an automated algorithm provided $v < 30$ cm/s. (Hence, lower velocities are used when velocity measurements are desired, as in Figs. 3–5.) Three images of the particles separated by 42 ms are acquired, and the positions of the corresponding particles are determined in each one. To identify corresponding particles in the different frames, the algorithm searches first for particles that move the least between the first and second frames. The third frame is used both as a check to eliminate erroneous matches and to improve the accuracy. We have found this method to work for 90% of the particles, provided that the interframe displacement is less than the typical nearest neighbor distance. The remaining particles are missed; this leads to an underestimate of the number of fast particles.

Using this technique, speed distributions $P(v)$ were determined in the range $100 < N < 1860$ for $\theta = 0.22^\circ$, but the results are expected to be similar for smaller θ . Figure 5(a) shows $P(v)$ for $n = 100, 500$, and 1860. The mean velocity decreases with increasing N , with most of the particles being nearly at rest, and a small number of “hot” particles with large velocities. These fast particles are located preferentially in low density regions, and their relative number declines with increasing N because of the strong dissipation produced by the

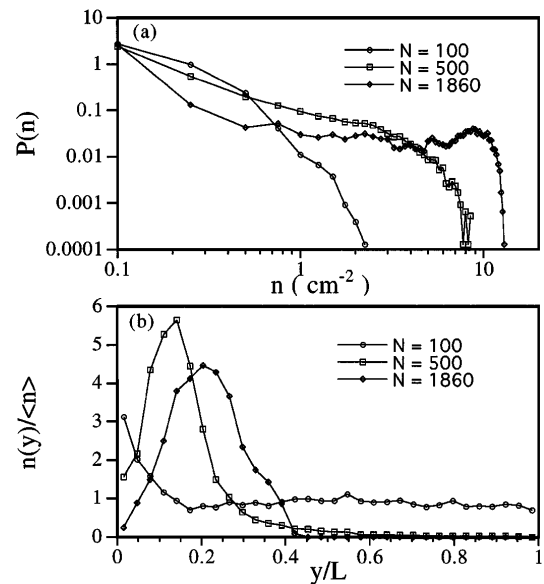


FIG. 4. (a) Density distributions $P(n)$ and (b) spatial density variation $n(y)$ for $\theta = 0.22^\circ$, as in Fig. 3. The particles cluster near the driving wall.

cluster. The number of hot particles may be somewhat augmented by the presence of instabilities, as this provides regions of lower density through which energy can be transmitted.

The mean collision rate $R(y)$ is highly inhomogeneous when a cluster is present. Even though the velocities are reduced within the clusters, the collision rate is much greater there. We determine $R(y)$ from the ratio $v(y)/\ell(y)$, where the mean free path $\ell(y)$ is determined from the measured density $\rho(y)$ [7]. The resulting col-

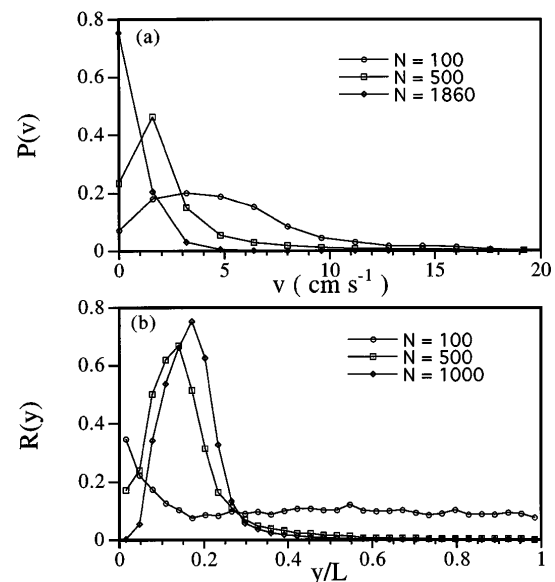


FIG. 5. (a) Speed distribution $P(v)$ for several values of N . The mean velocity decreases with increasing N . (b) The collision rate $R(y)$ as a function of distance from driving wall becomes strongly inhomogeneous at high N . ($\theta = 0.22^\circ$.)

lision rate is displayed in Fig. 5(b) for several values of N . For large N the collision rate is substantially enhanced within the clusters. Note that the peak in $R(y)$ is closer to the wall than is the peak in the density distribution.

A qualitatively similar observation of clustering (in 2D) away from the energy source (as in Figs. 1 and 2) was made in the numerical and theoretical work of Grossman, Zhou, and Ben-Naim [7], who explain clustering for $1 - r \ll 1$ by assuming an energy balance argument and local "thermal" equilibrium. However, there are significant differences between the model and this experiment. The theoretical work does not include particle rotation. Though it is reasonable to ignore the sharing of energy between rotation and translation at the instant of collision, rotation produces an effectively smaller coefficient of restitution in the experiment by the following mechanism. The particles are rolling at the instant of collision. After the collision, particle spin produces relative motion with respect to the surface. The resulting frictional slipping leads to additional dissipation until the rolling condition is restored over a distance of several mm. We determined experimentally that the *effective* coefficient of restitution (including this additional loss to the surface) is about 0.7 on average. However, it varies over the range $0.5 < r < 0.9$, with the larger values applying to grazing collisions and smaller values to backscattering or collisions with the wall. The approach of Ref. [7] is not quantitatively applicable for values of r this far from unity. However, the behavior of the density $n(y)$ shown in Fig. 2(b) is qualitatively similar to that given in Ref. [7].

We explored the role of weak gravitation numerically by generalizing the one dimensional model of Ref. [6]. The values of r , N , and θ were chosen to be appropriate for the experiment. Without gravity, the particles cluster at the side opposite to the driving wall as in Ref. [6] for 1D and in Ref. [7] for 2D. For $\theta = 0.22^\circ$, the simulation shows clustering near the driving wall for 10 particles, and no aggregation for 3 particles. These numbers correspond to 1000 and 300 particles, respectively, in 2D. (Corresponding cases would have the same numbers of particles along a line perpendicular to the forcing wall.) The computed density $n(y)$ is shown for these cases in Fig. 6; the results are qualitatively similar to what is found experimentally (see Fig. 4). Numerically, the cluster shifts from one wall to the other at a remarkably small angle (below 0.005°). Experimentally this critical angle is somewhat larger (about 0.1°) because of friction with the surface. Finally, we note that vertically oriented 1D granular media have been studied both experimentally and numerically [11].

In conclusion, density and velocity distributions, and spatially resolved density profiles and collision rates, all show pronounced effects due to clustering at high particle number. We do not see evidence of the stringlike clusters seen in numerical simulations of transient decay; they may not be present when energy is injected continuously,

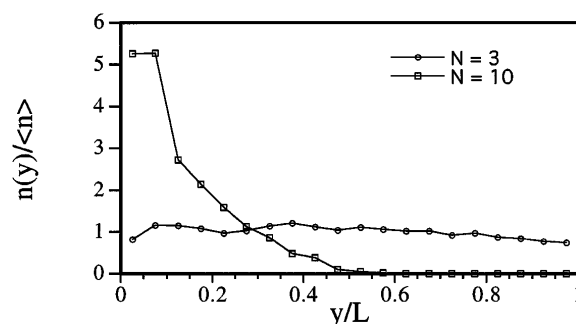


FIG. 6. Numerical simulation of a one dimensional model including gravitation for $\theta = 0.22^\circ$ and $r = 0.7$. The cases $N = 3$ and $N = 10$ correspond to 300 and 1000 particles in two dimensions. The spatial density variation $n(y)$ is similar to that seen experimentally in Fig. 4(b), with clustering near the driving wall.

as in this experiment. Experiments were performed with reduced L , with both larger and smaller particles (1.6–4.5 mm), and with higher forcing amplitude and/or frequency. The resulting behavior is qualitatively similar to that presented here. Many variants of these experiments are possible. For example, mixtures of particles of different densities and coefficients of restitution could lead to insight concerning particle segregation phenomena.

We wish to thank E. Grossman and L. Kadanoff for useful discussions and B. Boyes for technical assistance. This work was supported by NSF Grant No. DMR-9319973 and an equipment grant from the Zimmer Foundation.

- [1] C. S. Campbell, *Annu. Rev. Fluid Mech.* **22**, 57 (1990).
- [2] H. M. Jaeger, S. R. Nagel, and R. P. Behringer, *Phys. Today* **49**, No. 4, 32 (1996).
- [3] S. McNamara and W. R. Young, *Phys. Fluids A* **4**, 496 (1992).
- [4] S. McNamara and W. R. Young, *Phys. Rev. E* **50**, R28 (1994).
- [5] I. Goldhirsh and G. Zanetti, *Phys. Rev. Lett.* **70**, 1619 (1993).
- [6] Y. Du, L. Hao, and L. P. Kadanoff, *Phys. Rev. Lett.* **74**, 1268 (1995).
- [7] E. L. Grossman, T. Zhou, and E. Ben-Naim, *Phys. Rev. E* (to be published).
- [8] F. Melo, P. B. Umbanhowar, and H. L. Swinney, *Phys. Rev. Lett.* **75**, 3838 (1995).
- [9] E. E. Ehrichs *et al.*, *Science* **267**, 1632 (1995).
- [10] O. Zik, D. Levine, S. G. Lipson, S. Shtrikman, and J. Stavans, *Phys. Rev. Lett.* **73**, 644 (1994).
- [11] S. Luding, E. Clement, A. Blumen, J. Rajchenbach, and J. Duran, *Phys. Rev. E* **49**, 1634 (1994).
- [12] Garolite is used because of its light weight and high impact strength.
- [13] S. Douady, S. Fauve, and C. Laroche, *Europhys. Lett.* **8**, 621 (1989).
- [14] E. Clement, L. Vanel, J. Rajchenbach, and J. Duran, *Phys. Rev. E* **53**, 2972 (1996).